A robust nanoscale RP HPLC-MS approach for sensitive Fc proteoform profiling of IgG allotypes

Blöchl, C.; Gstöttner, C.; Sénard, T.; Stork, E.M.; Scherer, H.U.; Toes, R.E.M.; ... ; Domínguez-Vega, E.

Analytica Chimica Acta 1279 (2023) 341795

Contents lists available at ScienceDirect

Analytica Chimica Acta

journal homepage: www.elsevier.com/locate/aca

A robust nanoscale RP HPLC-MS approach for sensitive Fc proteoform profiling of IgG allotypes

Constantin Blöchl [a], Christoph Gstöttner [a], Thomas Sénard [a,1], Eva Maria Stork [b], Hans Ulrich Scherer [b], Rene E.M. Toes [b], Manfred Wuhrer [a], Elena Domínguez-Vega [a,*]

[a] Center for Proteomics and Metabolomics, Leiden University Medical Center, Albinusdreef 2, 2333 ZA, Leiden, the Netherlands
[b] Department of Rheumatology, Leiden University Medical Center, Albinusdreef 2, 2333 ZA, Leiden, the Netherlands

HIGHLIGHTS

- Development of a nano RP HPLC-MS approach for intact Fc/2 of polyclonal IgG.
- Glycoform profiling in a fully subclass- and allotype-specific manner.
- Accessibility of Fc proteoforms beyond bottom-up analysis.
- Semi-automated data analysis workflow for intact Fc/2 subunits.
- Robustness, sensitivity, and throughput suitable for clinical cohorts.

GRAPHICAL ABSTRACT

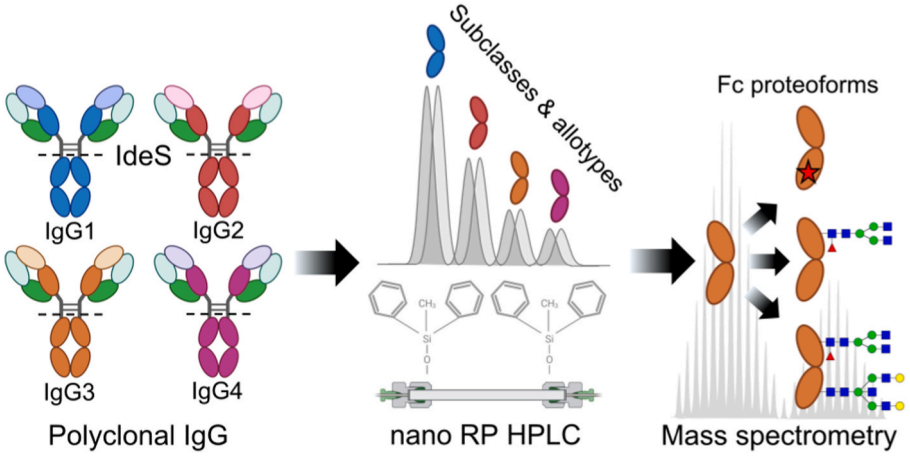

ARTICLE INFO

Handling Editor: Dr. L. Liang

Keywords:
Polyclonal immunoglobulin G
Antibodies
Subclasses
Glycosylation
Post-translational modifications

ABSTRACT

The conserved region (Fc) of IgG antibodies dictates the interactions with designated receptors thus defining the immunological effector functions of IgG. Amino acid sequence variations in the Fc, recognized as subclasses and allotypes, as well as post-translational modifications (PTMs) modulate these interactions. Yet, the high similarity of Fc sequences hinders allotype-specific PTM analysis by state-of-the-art bottom-up methods and current subunit approaches lack sensitivity and face co-elution of near-isobaric allotypes.

To circumvent these shortcomings, we present a nanoscale reversed-phase (RP) HPLC-MS workflow of intact Fc subunits for comprehensive characterization of Fc proteoforms in an allotype- and subclass-specific manner. Polyclonal IgGs were purified from individuals followed by enzymatic digestion releasing single chain Fc subunits (Fc/2) that were directly subjected to analysis. Chromatographic conditions were optimized to separate Fc/2 subunits of near-isobaric allotypes and subclasses allowing allotype and proteoform identification and

* Corresponding author.
E-mail address: e.dominguez_vega@lumc.nl (E. Domínguez-Vega).
[1] Present address: Ludger Ltd., Culham Science Centre, OX14 3EB Abingdon, United Kingdom.

https://doi.org/10.1016/j.aca.2023.341795
Received 29 June 2023; Received in revised form 30 August 2023; Accepted 6 September 2023
Available online 9 September 2023

quantification across all four IgG subclasses. The workflow was complemented by a semi-automated data analysis pipeline based on the open-source software Skyline followed by post-processing in R. The approach revealed pronounced differences in Fc glycosylation between donors, besides inter-subclass and inter-allotype variability within donors. Notably, partial occupancy of the *N*-glycosylation site in the C_H3 domain of IgG3 was observed that is generally neglected by established approaches. The described method was benchmarked across several hundred runs and showed good precision and robustness.

This methodology represents a first mature Fc subunit profiling approach allowing truly subclass- and allotype-specific Fc proteoform characterization beyond established approaches. The comprehensive information obtained paired with the high sensitivity provided by the miniaturization of the approach guarantees applicability to a broad range of research questions including clinically relevant (auto)antibody characterization or pharmacokinetics assessment of therapeutic IgGs.

1. Introduction

Immunoglobulin G (IgG) antibodies are key effector proteins of the immune system responsible for the clearance of exogenous and endogenous agents. While the variable fragment antigen-binding (Fab) part is responsible for antigen recognition, the conserved fragment crystallizable (Fc) region translates effector signals by binding to downstream receptors, e.g., Fc gamma receptors [1]. The specific amino acid sequence of the Fc region determines the subclass of IgG, i.e., IgG1-4, as well as its allotype [2] and is a major determinant of the IgG's ability to activate biological signaling pathways, e.g., antibody-dependent cellular cytotoxicity (ADCC) [3] or complement-dependent cytotoxicity (CDC) [2]. In addition to manifold sequence variations, post-translational modifications (PTMs) such as glycosylation or oxidation, significantly alter binding to these receptors [4–6]. Alterations in the PTM profiles of endogenous IgG have been reported in a number of diseases, including autoimmunity [7], are linked to disease severity, and have been proposed as clinical biomarkers [8]. In addition, Fc glycosylation is linked to the physiological state of an organism and changes for instance during pregnancy or with age [8].

Given the biological importance of IgG and its molecular characteristics, dedicated analytical methods have been developed. Among these, approaches for the analysis of the Fc glycans are by far the most widespread and rely mainly on released glycan or glycopeptide analyses [9]. However, these (bottom-up) methods are generally targeted at specific subclasses or PTMs rendering them blind for many IgG sequence variations or co-occurring modifications. In addition, common IgG2 and IgG3 allotypes yield identical tryptic glycopeptides thus requiring dedicated sample preparation strategies [10]. Similarly, IgG3 and IgG4 may share isomeric tryptic glycopeptides depending on the specific allotypes [11]. Yet, subclass-specific glycosylation analysis is of high relevance as glycosylation patterns differ significantly between subclasses [12].

Driven by methodological and technical advancements, intact protein analysis is gaining interest as holistic analytical approach for the characterization of antibody biopharmaceuticals [13–16]. Since the great variability of the Fab domain hinders the analysis of intact polyclonal IgG, the conserved Fc region has to be released from intact IgG. This is, at present, achieved by either limited proteolysis, e.g., LysC [17], or specific enzymatic digestion, e.g., IdeS or SpeB [18–20], yielding single chain Fc subunits (Fc/2) – approaches recognized as middle-up/down. To our knowledge, characterization of polyclonal IgG from human individuals based on the intact Fc/2 subunit was so far pursued only by two studies. Goetze et al. [21] characterized Fc/2 subunits from several donors revealing IgG1 and IgG2 allotypes and their glycosylation profiles additionally leading to the identification of a previously undescribed IgG1 allotype. Although this study demonstrated the feasibility and capabilities of such an approach, it lacked both separation capabilities as well as sensitivity due to analytical scale column dimensions. Therefore, only IgG1 and IgG2 allotypes were amenable to this approach. Recently, Senard et al. further pursued this idea and applied capillary scale hydrophilic interaction liquid chromatography (HILIC) and capillary electrophoresis (CE) both coupled to mass spectrometry (MS) to separate and characterize Fc/2 subunits [22]. While this study could decrease limits of detection demonstrating the feasibility of assessing also lower abundant IgG3 and IgG4 allotypes, some prevalent allotypes were insufficiently separated by both HILIC-MS and CE-MS thereby limiting the applicability of these analytical approaches. In addition, the capillary scale of the HILIC approach as well as restricted injection volumes in CE, still provided limited sensitivity, which would be required for the analysis of, e.g., antigen-specific IgGs.

Here, we established a robust and sensitive nanoscale RP HPLC-MS approach dedicated to a comprehensive characterization of the intact Fc region of human polyclonal IgG. By achieving chromatographic resolution of critical IgG allotype pairs, we present an unbiased and comprehensive view on allotype proteoforms. The method shows high sensitivity making it applicable to minute sample amounts and low IgG concentrations. Together with its throughput and robustness, the analysis of patient cohorts consisting of hundreds of samples becomes feasible.

2. Materials and methods

2.1. Sample preparation

Fc/2 subunits of IgG allotypes were prepared based on a protocol previously described by Senard et al. [22] with a few minor amendments. Briefly, human plasma samples obtained from individual donors were diluted 1:8 in phosphate-buffered saline (PBS; 0.035 mmol·L^{-1} phosphate, 150 mmol·L^{-1} NaCl, pH 7.6) to an approximate concentration of 1.25 μg·μL^{-1} IgG calculated based on literature values of approx. 10 μg·μL^{-1} IgG in adults [23]. 6.4 μL of diluted plasma were further diluted to 100 μL in PBS and purified on 10 μL of Fc-specific agarose beads (CaptureSelect™ FcXL Affinity Matrix; Thermo Fisher Scientific, Waltham, MA) self-packed into 96-well filter plates (10 μm pore, Orochem Technologies, Naperville, IL). After an incubation step of 2.0 h at room temperature while shaking, all wells were washed four times with 200 μL PBS. In all cases, the supernatant was removed from the beads employing a centrifugation step at 500×*g* for 1 min. Subsequently, IgG was digested below the hinge region by applying the protease IdeS (Genovis, Lund, Sweden) at a ratio of 2 U·μg^{-1} IgG in 20 μL PBS. After incubation at 37 °C for 3.0 h in a moisture box, Fab subunits and IdeS were removed by centrifugation followed by another washing step (thrice with 200 μL of PBS and once with 200 μL of water). Finally, Fc subunits were eluted by incubation with 20 μl of 100 mmol·L^{-1} formic acid (FA; VWR Chemicals, Radnor, PA). The elution step was repeated once and the pooled eluates were directly subjected to HPLC-MS analysis. Fc/2 subunits of donors 2–4 were characterized by three independent purification procedures and measured in duplicates. Fc/2 subunits of donor 1 were purified once and measured in duplicates. System performance was monitored by an Fc/2 standard that was generated by digesting a commercial preparation of Trastuzumab (Herceptin; Roche Diagnostics GmbH, Penzberg, Germany) with IdeS (1 U·μg^{-1} IgG) in 150 mmol·L^{-1} ammonium acetate (Sigma-Aldrich) followed by a dilution in 150 mmol·L^{-1} ammonium acetate to a

concentration of 50 ng·μL^{-1}.

2.2. RP HPLC

Fc/2 subunits were analyzed on an U3000 nanoRSLC system (Thermo Fisher Scientific) equipped with a 5.0 μL sample loop. 0.75 μL and 1.00 μL of sample and Fc/2 standard, respectively, both corresponding to approx. 50 ng of Fc/2 subunits were injected in microliter pick-up mode onto a C4 trap column (5.0 × 0.3 mm i.d., Acclaim™ PepMap™, 300 Å pore size; Thermo Fisher Scientific) employing a flow rate of 15 μL·min^{-1} provided by the designated loading pump. Trapping of samples was conducted under isocratic conditions, i.e., H_2O + 0.1% trifluoroacetic acid (TFA; Merck, Darmstadt), at a temperature of 60 °C for 5 min. A forward-flow installation employing a 6-port switching valve was used for elution from the trap column onto the separation column. Separation of Fc/2 subunits was conducted on a diphenyl reversed phase column (150.0 × 0.1 mm i.d, Halo® Bioclass, 1000 Å pore size; Advanced Material Technology, Wilmington, DE) at a flow rate of 1.0 μL·min^{-1}. The separation column was located in an additional column oven (Butterfly heater; Phoenix S&T, Chadds Ford, PA) set to 80 °C. A shallow multi-step gradient employing solvent A (H_2O (ELGA Labwater, Ede, the Netherlands) + 0.1% TFA) and solvent B (acetonitrile (Actu-All Chemicals, Oss, the Netherlands) + 0.1% TFA) was programmed as follows: 20.0% B for 5 min, 20.0%–33.5% in 1.0 min, 33.5–35.0% B in 12 min, 35.0–60.0% B in 2 min, 90.0% B for 5 min, and 20% B for 5 min.

2.3. Mass spectrometry

The HPLC system was coupled to a qTOF mass spectrometer (Maxis HD) *via* a nano-ESI source (CaptiveSpray; both from Bruker, Bremen, Germany). Acetonitrile-enriched nitrogen gas was employed at a pressure of 0.40 bar (nanoBooster system; Bruker). Additionally, drying gas flow was set to 3.0 L/min at a temperature of 220 °C. The system was operated in positive mode with a spray voltage of 1000 V. Collision cell RF was set to 2000 Vpp, the quadrupole ion and collisions cell energies were 5.0 and 7.0 eV, respectively, the pre-pulse storage was put to 20.0 μs, and the transfer time to 150.0 μs. Funnel 1 and funnel 2 RF were 300.0 and 600.0 Vpp, respectively. An in-source CID of 65 eV provided sufficient de-clustering potential without fragmentation of our analytes. The mass range was set from *m/z* 600-4000 including a rolling average of three scans resulting in an acquisition rate of 1.0 Hz.

2.4. Data evaluation

Initial identification of allotypes was based on protein average masses acquired by deconvolution of raw mass spectra. Deconvolution was achieved by the maximum entropy algorithm implemented in the Compass DataAnalysis software (Bruker). To achieve optimal deconvolution, the resolution was set to 5000 and the data spacing to 1.0, followed by mass picking based on the Sum Peak algorithm also embedded in the Compass DataAnalysis software package. Subsequently, identification and relative quantification of allotypes and their proteoforms was conducted in Skyline (version 22.2.0.351) relying on extracted ion current chromatograms (EICCs) [24]. Prior to data import, raw mass spectra were converted into the open source mzml format only including time points 600–1320 s and *m/z* 1000 to 1600 to limit processing and evaluation time as well as saving space for data storage employing msConvert [25]. mzml files were further processed within the OpenMS software environment initially applying Gaussian smoothing of individual mass spectra (default settings, peak width of *m/z* 1.0) followed by a baseline subtraction in these processed mass spectra with the Tophat algorithm (default settings, width *m/z* 1.0) [26]. Finally, files were imported into the Skyline software for proteoform identification and quantification. Assignment and subsequent relative quantification were based on matching *m/z* as well as expected retention times. The most abundant charge state (19+) and the two adjacent charge states (18+ and 20+) were used for generating EICCs using the most abundant isotope, which was automatically calculated by Skyline for each charge state. The extraction width was also automatically determined given a TOF resolution setting that was put to 15,000. EICCs were automatically integrated by Skyline and curated manually. The exported report was further processed within the R programming environment [27]. Of note, IgG3 allotypes that show occupancy of both *N*-glycosylation sites were quantified after deconvolution. Data visualization and statistical assessment was partly conducted in GraphPad Prism 9.3.1.

2.5. Allotype- and Glycan-nomenclature

Allotypes were labeled based on the nomenclature proposed by Lefranc and Lefranc referred to as IMGT accession numbers in this study [28]. In principle, allotypes are denoted, e.g., as IGHG1*01, where the first number identifies the subclass and the second number the specific allotype number. Sequences were retrieved from the associated website imgt.org. Throughout this manuscript, annotation of allotypes was conducted by showing only the first matching allotype number given the fact that several IMGT amino acid sequences are identical or isobaric. An overview of considered sequences is available in Supplementary Table S1. Based on an established nomenclature, glycans were named by adding galactose (G), fucose (F), bisecting *N*-acetylglucosamine (GlcNAc; N), and *N*-acetylneuraminic acids (S) to the core glycan structure of the complex type, e.g., G2F for a doubly galactosylated and core fucosylated glycan.

2.6. Informed consent

All donors included in the study gave written informed consent for sample acquisition. The study was approved by the medical ethical review board of the Leiden University Medical Center under code P17.151.

2.7. Data availability

The raw mass spectrometry data is available under: https://doi.org/10.5281/zenodo.7852039.

3. Results

3.1. Separation and identification of Fc/2 subunits

Polyclonal IgG from individual donors were purified from plasma using Fc-specific beads followed by on-bead below-hinge-region digestion by IdeS as described previously (Fig. 1a) [22]. While Fab portions could be washed from the beads at a neutral pH, desired Fc/2 subunits were eluted from the beads under acidic conditions (0.1 mol·L^{-1} formic acid) and directly injected for nano RP HPLC-MS analysis without any additional sample treatment. To achieve robustness as well as sensitivity, a forward-flow trap set-up was chosen: while a short trap column operated at high flow rates (15 μL·min^{-1}) provided tolerance for less pure samples, e.g., salts, the separation was conducted on a nano column to maximize sensitivity. As sensitivity is directly associated with flow rate, a small column diameter (100 μm i.d.) was selected permitting to reduce the flow rate to 1 μL·min^{-1} providing higher sensitivity than current Fc/2 HPLC-MS approaches [21,22]. MS conditions were optimized using an Fc/2 standard (IGHG1*03) obtained from digestion of a commercial preparation of trastuzumab. Adding acetonitrile as dopant solvent to the nitrogen gas aided electrospray ionization and led to a significant hyper-charging effect moving the most abundant charge state from 15+ to 19+ (Supplementary Fig. S1). Adduct formation was found unaltered upon enrichment of the nitrogen gas with acetonitrile within the same charge state. Still, the hyper-charging effect was indirectly beneficial for the analysis, as charge states <14+ showed pronounced formation of TFA adducts compared to higher charge states. In addition,

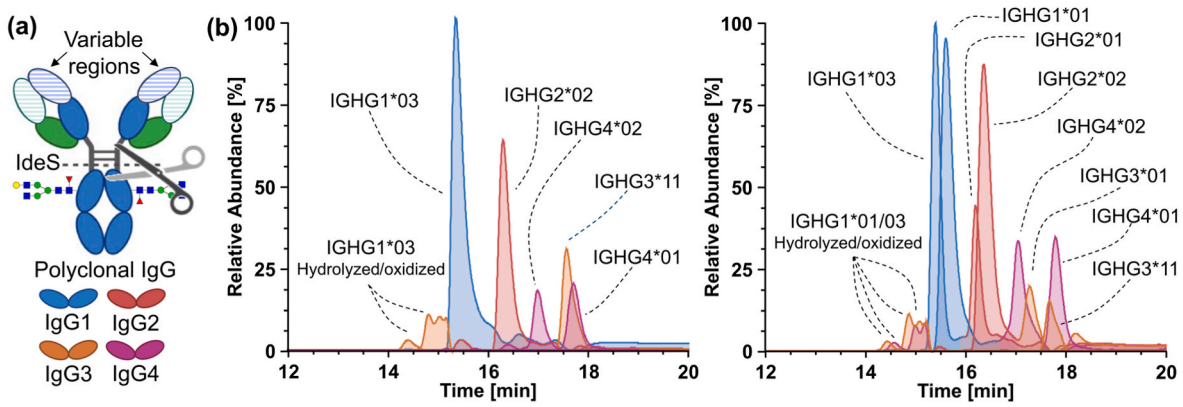

Fig. 1. Analysis of Fc/2 subunits released from polyclonal IgG by RP HPLC-MS. (a) Schematic of an IgG1 antibody that is digested by IdeS below its hinge region releasing Fc/2 subunits. The heavy chain is indicated in blue and the light chain in green, whereas conserved and variable regions are colored in darker and lighter shades, respectively. The color code for IgG subclasses (blue-IgG1, red-IgG2, orange-IgG3, and purple-IgG4), which is used throughout this manuscript, is indicated. (b) Combined EICCs reveal allotype profiles of two individual donors. Donor 1 (left panel) is homozygous for IgG1, IgG2, and IgG3 allotype sequences. However, two IgG4 sequences are observed. Donor 2 (right panel) is heterozygous for all four subclasses, thus displaying eight allotype sequences. In addition, oxidized and hydrolyzed IGHG1 peaks are annotated that were co-extracted during EICC generation. The 19+ charge state of the G1F glycoform is shown in all cases. (For interpretation of the references to color in this figure legend, the reader is referred to the Web version of this article.)

acetonitrile led to a significant reduction of noise levels in the region $< m/z$ 1000. Overall, this resulted in a significant gain in sensitivity compared to existing methods [21,22] allowing routine analysis from approx. 150 ng of IgG per injection, which makes low abundant, yet highly relevant subpools of IgG accessible, e.g., autoantibodies [29] or therapeutic antibodies during pharmacokinetics studies [30]. Compared to the previously published HILIC-MS method [22] (1,660 ng polyclonal IgG per run) and a RP HPLC-MS approach for murine IgG [19] (3,000 ng polyclonal IgG per run) sensitivity could be increased roughly 10- and 20-fold, respectively.

The chromatographic method was carefully optimized to separate critical near-isobaric allotype pairs (Supplementary Fig. S2). Of note, these pairs are co-extracted during EICC generation due to a large overlap of their isotopic distributions rendering the chromatographic separation essential for identification and quantification. Eventually, the desired chromatographic separation was achieved by a high separation temperature (80 °C) paired with a phenyl-selectivity of the stationary phase and a very shallow gradient. Importantly, for the first time, the highly prevalent allotype pair IGHG1*03 and IGHG2*01 was clearly separated, which could not be achieved by previous studies: both Goetze et al. [21] and Senard et al. [22] could only obtain a partial separation by analytical RP HPLC and CE, respectively, making quantification difficult and error-prone. Besides the near-isobaric allotype-pair IGHG1*01-IGHG4*02, also IGHG2*02-IGHG3*01 and IGHG3*11-IGHG3*16, which show significant co-extraction at EICC level, could be separated (Supplementary Fig. S2). These four pairs constitute the most problematic allotypes in terms of isobaricity and are highly prevalent in Caucasoid and Mongoloid populations [2,31]. Notably, we could only obtain partial separation of IGHG2*01/IGHG2*02 and IGHG3*11/IGHG4*01 allotypes, respectively, which partially overlap in the isotopic distribution of non-bisected and bisected glycans. The obtained partial separation allowed identifying these allotypes and subsequently adapting their EICC windows. These adjustments of EICC windows of affected glycoforms towards a selective extraction resolved the co-extraction issue and allowed their independent relative quantification in both cases (Supplementary Fig. S3). For relative quantification, peak area compensation factors were included in the data analysis workflow, which are based on the ratio of peak areas (original EICC window vs. adapted EICC window) of the unbiased G0F glycoform as explained in detail in Supplementary Table S2.

After separation of these allotypes was achieved, four individual donors were investigated for their allotype constitution (donors 1–4; Supplementary Table S3). The combined EICCs of the G1F glycoform for the identified allotypes is depicted for donor 1 and donor 2, respectively (Fig. 1b). While donor 1 was homozygous for all IgG subclasses except IgG4, donor 2 revealed heterozygosity for all IgG subclasses. Generally, IgG1 allotypes eluted first, followed by IgG2 allotypes. IgG3 and IgG4 allotypes eluted later, whereas their order was dependent on the specific allotype. Since allotypes are generally inherited in a fixed combination referred to as haplotypes, confident identification of one allotype can be harnessed to identify genetically connected allotypes [2,31]. This is especially helpful if information about the ethnicity of the donors is available. A table depicting prevalent haplotypes in the respective populations and the linked allotypes including IMGT accession numbers was compiled (Supplementary Table S4). Haplotypes were assessed for all donors and found to be mainly of Caucasian descent (Supplementary Table S3). Yet, every donor showed a distinct haplotype profile illustrating the genetic diversity in the population. For instance, haplotypes of donors depicted in Fig. 1b were found to be G3m5*; G1m3; G2m23 (donor 1, homozygous) and G3m5*; G1m3; G2m23/G3m5*; G1m17,1; G2m.. (donor 2, heterozygous). Yet, it should be noted that one allotype may be represented by different IMGT accession numbers. Experimental masses for all identified allotypes as well as corresponding mass errors are provided in Supplementary Table S5.

Interestingly, oxidized and hydrolyzed forms of IgG1 allotypes were found at the start of the gradient (Fig. 1b, Supplementary Fig. S4). Oxidation of Fc/2 is likely present on two well-studied methionines, e.g., M256 and M432 for IgG1, which may be oxidized *in vivo* and/or during prolonged sample storage [32]. Multiple peaks of oxidized Fc/2 likely result from oxidation of either one of the two methionine residues, which can be separated by RP chromatography as demonstrated for the Fc domain of biopharmaceuticals [33]. Hydrolyzed forms are likely an analytical artefact caused by hydrolysis between aspartic acid and proline under the acidic conditions and high temperature employed during separation [34]. The presence of such hydrolyzed forms during analysis of Fc/2 by RP HPLC was reported earlier [21] and highlights the benefit of analyzing non-reduced Fc/2 as the disulfide bonds keep the cleaved polypeptide chains connected. In addition, early eluting species included a truncated version of Fc/2 of low abundance (<1%), likely due to hydrolysis after an aspartic acid in the N-terminal region (Supplementary Fig. S5). As this site is in close vicinity to the first cleavage site of IdeS and the aspartic acid – threonine bond is less prone to hydrolysis, potentially an additional minor cleavage site of IdeS would be imaginable.

3.2. Assessing Fc Glyco- and proteoforms

The developed HPLC-MS method allowed assessment of Fc glycoforms in a truly subclass- and allotype-specific manner. This overcomes the issue of identical IgG2 and IgG3 glycopeptides as well as isobaric IgG3 and IgG4 glycopeptides encountered in bottom-up approaches [10,11]. Notably, the prevalence of these problematic peptides is depending on the allotype constitution of an individual and is associated with the population investigated (Supplementary Tables S1 and S4).

Generally, the retention time of Fc/2 is mainly governed by the amino acid sequence resulting in co-elution of glycoforms of the same allotype in the applied RP HPLC approach (Fig. 2a). This renders assignment of glycoforms to the respective allotype straight-forward compared to other approaches such as HILIC, where both amino acid sequence as well as the glycan portion have an influence on the retention time [22]. Also, CE-based separation was shown to be generally driven by the Fc/2 amino acid sequence although resolution was generally lower than currently achieved with the RP HPLC method [22]. Besides, negatively charged glycans have significant influence on the electrophoretic mobility, adding complexity to the profiles. While the glycan composition of singly-glycosylated Fc/2 had negligible influence on the retention time, non-glycosylated Fc/2 was more hydrophobic resulting in a pronounced retention time shift as exemplarily visualized for an IgG3 allotype in Fig. 2b. Intriguingly, we also observed partial occupancy of the second *N*-glycosylation site in the C_H3 domain of IgG3 at Asn392 (Fig. 2b). The presence of two *N*-glycans led to a shift in retention time towards earlier elution. To better visualize the elution patterns of these species, the lower abundant G0FN glycoform was selected for the singly glycosylated Fc/2, which allows comparison with the abundance of the doubly and non-glycosylated Fc/2 (Fig. 2b). A similar comparison using the most abundant glycoform (G0F) of the singly glycosylated Fc/2 is depicted in Supplementary Fig. S6. The deconvoluted mass spectra of IgG3 peaks showing these differences in glycan site occupancy are presented in Fig. 2c. C_H3 domain glycans were strikingly different from those of the conserved C_H2 domain. In contrast to lowly sialylated core fucosylated complex type glycans in the C_H2, C_H3-associated glycans were dominated by afucosylated and highly bisected complex type glycans. In addition, an abundant oligomannose type glycan was identified. Considering the C_H2 glycan distribution was unaffected by C_H3 glycans, C_H3 glycans clearly matched those identified earlier by Stavenhagen et al. using a dedicated RP-porous graphitized carbon HPLC-MS approach [35]. Glycoforms showing both *N*-glycosylated C_H2 and C_H3 domains were quantified as well as the fractions of none, singly, and doubly glycosylated Fc/2 (Supplementary Fig. S7). Corresponding data is listed in Supplementary Table S6 for all donors investigated. C_H3 domain glycosylation of IgG3 is generally neglected in established bottom-up approaches and requires tailored analytical workflows [35]. The developed approach provides information on the co-occurrence of C_H2–C_H3 glycoforms beyond a stochastic combination as provided by bottom-up approaches. Compared to these approaches, our analytical strategy enables analysis of differentially occupied Fc/2 subunits that share the identical and relatively big protein backbone rendering MS response factors potentially less biased by glycosylation. Additionally, within glycoforms, negatively charged sialic acid residues

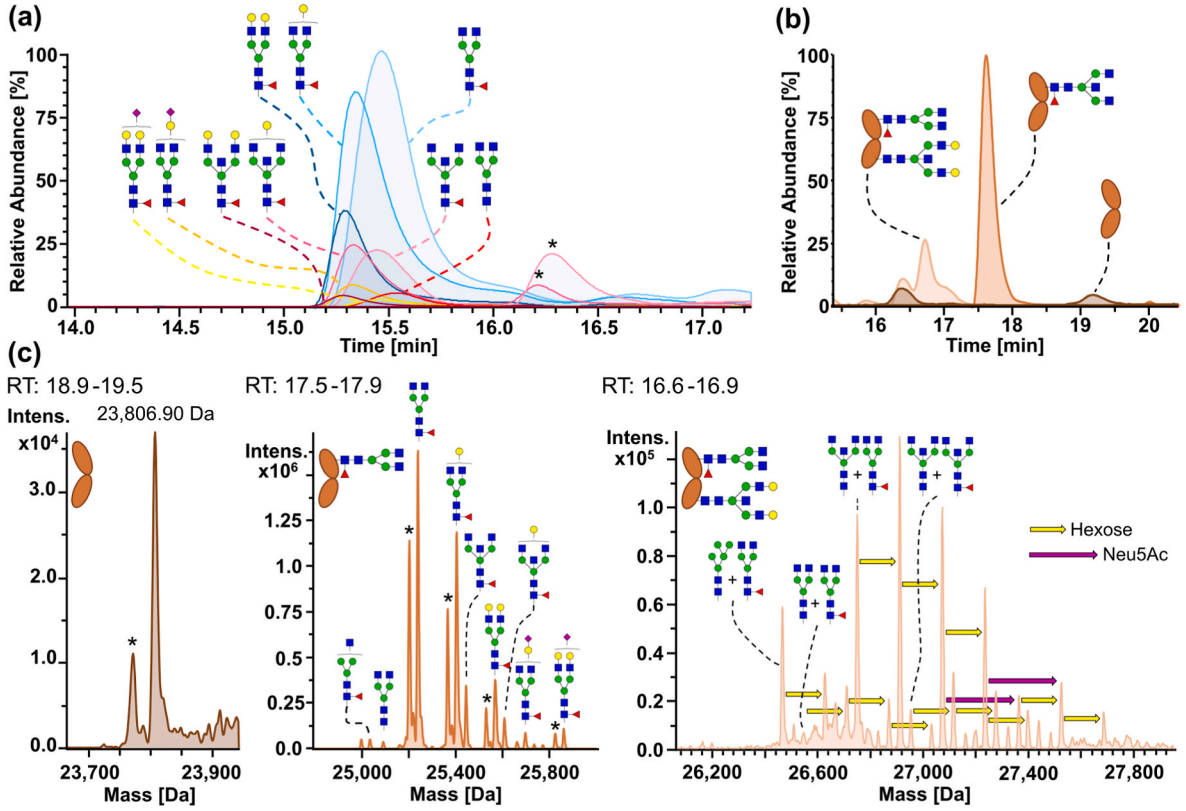

Fig. 2. Characterization of Fc-associated glycoforms. (a) Combined EICCs of the main glycoforms present on IGHG1*03. EICCs were generated using the 19+ charge state for every glycoform. Non-bisected fucosylated neutral glycans are labeled in shades of blue, bisected neutral glycans in shades of pink, afucosylated neutral glycans in red, and acidic glycans in yellow/orange. Asterisks (*) denote co-extracted glycoforms of IGHG2*02. (b) Separation of Fc/2 subunits of the IGHG3*11 allotype bearing either none, one, or two *N*-glycans. (c) Deconvoluted mass spectra of the non-glycosylated (left panel), singly glycosylated (middle panel), and doubly glycosylated Fc/2 (right panel) of IGHG3*11. Glycoforms of the doubly glycosylated Fc/2 are annotated starting from four non-galactosylated glycoforms. Additions of hexoses (yellow arrow, +162 Da) and *N*-acetylneuraminic acid (Neu5Ac; purple arrow, +291 Da) to these annotated glycoforms are indicated. Asterisks (*) denote co-eluting glycoforms of IGHG4*01. Presented data was acquired from donor 1. (For interpretation of the references to color in this figure legend, the reader is referred to the Web version of this article.)

have less influence on the ionization of proteins compared to peptide-based bottom-up approaches [36,37].

In addition to glycosylation, oxidation, and hydrolysis, we observed glycation of the Fc/2. Although glycation is isobaric to mass shifts that are caused by the addition of galactose residues to complex type glycans, we focused on a comparison between the fully galactosylated G2F and the glycated G2F proteoform (Supplementary Fig. S8). Accurate determination of glycation levels could be further achieved by prior deglycosylation by, e.g., PNGase F or EndoS [21]. Glycation of endogenous IgG in healthy individuals has been reported to be ranging from 1 to 5 glucose molecules [38] or around 7% for intact IgG [39]. Our methodology mainly revealed singly glycated Fc/2 of varying abundance. Given the fact that glycation is predominantly found on the Fab regions [38,39] and considering that only Fc/2 subunits were examined by our approach, this amount of glycation seems reasonable.

Next, we quantified the identified Fc/2 variants encountered in the investigated donors and benchmarked the performance of the developed method. Generally, up to 13 glycoforms were observed per allotype resulting in 50–100 proteoforms per donor of greatly varying abundance to be quantified (Fig. 3). To streamline the EICC-based quantification of these manifold proteoforms, we established a semi-automated data analysis pipeline relying on the open-source software Skyline and post-processing within the R programming environment. This data evaluation strategy provided insightful visualization of the acquired data paired with reproducible integration of allotype proteoforms and quality control thereof, i.e., retention time, peak area, and mass error.

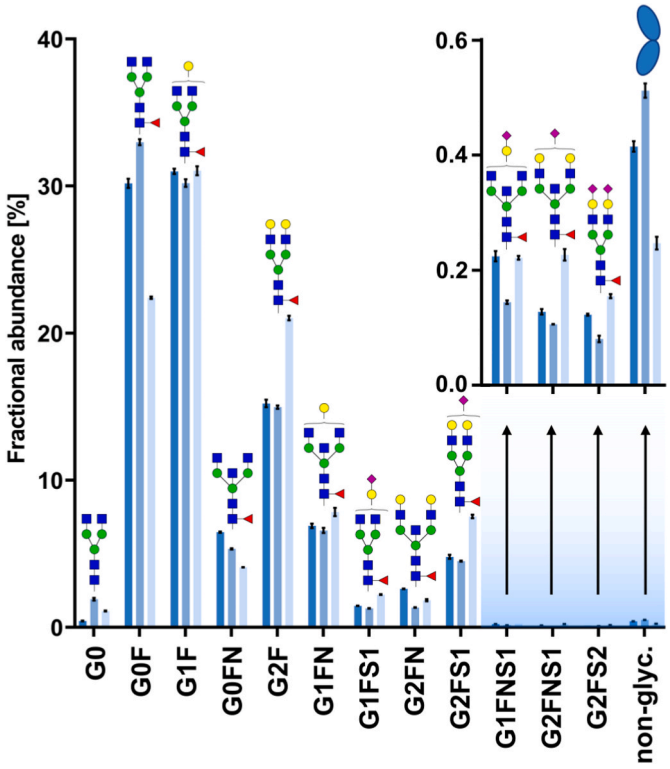

Fig. 3. Relative quantification of IGHG1*03 Fc-glycoforms across three donors. Thirteen (glyco)forms were detected and quantified. Glycoforms are listed by ascending molecular mass. The insert shows a zoom (0.0%–0.6% fractional abundance) into the last four analytes that were low in abundance. Individual donors are indicated in different shades of blue. Fractional abundances are depicted as mean values based on three independent technical replicates of which each replicate was averaged from duplicate HPLC-MS measurements. Standard deviations are indicated. The overall relative standard deviation was 2.05% across these three donors (donors 2–4). (For interpretation of the references to color in this figure legend, the reader is referred to the Web version of this article.)

Initially, allotype (subclass) abundances and glycoforms of donor 2 presented in Fig. 1b were quantified (Supplementary Figs. S9 and S10). As anticipated, we observe a higher abundance of the IGHG2*02 allotype compared to IGHG2*01 [21,40]. Interestingly, we also see a minor difference in the prevalence of IGHG1*01 compared to IGHG1*03. Regarding glycosylation, as reported earlier, subclass-specific differences in Fc glycans were observed, e.g., higher levels of fucosylation of IgG2 compared to IgG1 [12]. In addition, we detected allotype-specific differences, e.g., significantly higher levels of bisection of IGHG1*03 compared to IGHG1*01 (Supplementary Fig. S11). Afucosylation and galactosylation of IGHG3*01 was also higher compared to IGHG3*11 (Supplementary Fig. S10). Evidence for allotype-specific glycan profiles has been suggested especially for IgG3 allotypes [3]. Yet, these results are based on monoclonal antibodies produced in HEK 293F cells. Analysis of single-donor polyclonal samples eliminates cell culture-related glycosylation variability and provides improved comparison on changes associated to allotype variations. Furthermore, pronounced inter-donor variability was detected within the same allotype. Glycan patterns of donors 2–4 were quantified exemplarily for IGHG1*03 (Fig. 3) and further visualized as derived glycan traits (Supplementary Fig. S11): non-galactosylated glycans spanned from 26.56% to 38.38%, non-fucosylated glycans from 0.44% to 1.92%, and sialylated glycans from 6.08% to 10.33%. Qualitative and quantitative data on glycoforms of all allotypes from donors 2–4 as well as (relative) standard deviations are shown in Supplementary Tables S7–S9.

To assess the performance of the whole workflow, we assessed precision in a set of three donors focusing on the IGHG1*03 allotype (Fig. 3). Throughout the three donors, we quantified 12 glycoforms as well as the non-glycosylated Fc/2 from only about 50 ng of Fc/2 (combined for all allotypes). Based on reported subclass distributions [23] this translates to about 14 ng of IGHG1*03 Fc/2. Low abundant glycoforms (<0.6% fractional abundance corresponding to 0.08 ng) could still be quantified with reasonable standard deviations (Fig. 3). Standard deviations within donors were generally reasonable with an average relative standard deviation (RSD) of 2.05%. Moreover, performance of the nanoscale HPLC-MS system was assessed by repetitive measurement of the described Fc/2 standard. In essence, the developed method was employed to measure Fc/2 obtained from donors continuously for more than 7 days (367 runs). Throughout this series of measurements, critical parameters, i.e., relative abundance, retention time, and peak width of the G0F variant as well as G0 abundance, were monitored by Shewart control charts (Supplementary Fig. S12). All monitored values stayed within the warning intervals demonstrating the robustness of the method.

4. Conclusions

We sought to advance IgG antibody analysis by achieving full subclass- and allotype-resolution for comprehensive Fc glyco- and proteoform profiling. The approach overcomes the issue of identical and isobaric glycopeptides that usually limits informative value of bottom-up methods. In addition, the method makes Fc modifications accessible that are currently neglected or not accessible in a subclass-specific manner by established approaches as demonstrated for C_H3 glycosylation and glycation. The main shortcomings of comparable methods, namely sensitivity, co-elution of near-isobaric allotypes, and the bottleneck of data evaluation could be largely overcome. The wealth of data that can be retrieved within a single HPLC-MS run was demonstrated for a panel of four donors. Employing quality control samples, we benchmarked the approach across several hundred runs, demonstrating its robustness, precision, and applicability for high-throughput analysis. Given its miniaturization, the approach lends itself to the analysis of minute samples or subpools of IgG ensuring applicability to a broad spectrum of clinical questions. We envision profiling of disease-associated IgG proteoforms for instance in autoimmunity, characterized by pro-inflammatory Fc modifications, or metabolic diseases, where

novel Fc modifications are introduced – both are scenarios where a holistic approach is key to understand the immunological implications of IgG proteoforms translated by its very Fc region.

CRediT authorship contribution statement

Constantin Blöchl: Conceptualization, Software, Formal analysis, Investigation, Data curation, Writing – original draft, Writing – review & editing, Visualization. **Christoph Gstöttner:** Investigation, Writing – review & editing. **Thomas Sénard:** Conceptualization, Writing – review & editing. **Eva Maria Stork:** Resources, Writing – review & editing. **Hans Ulrich Scherer:** Resources, Supervision, Writing – review & editing. **Rene E.M. Toes:** Resources, Supervision, Writing – review & editing. **Manfred Wuhrer:** Conceptualization, Resources, Supervision, Writing – review & editing. **Elena Domínguez-Vega:** Conceptualization, Resources, Supervision, Project administration, Funding acquisition, Writing – review & editing, All authors agreed to the final version of the manuscript.

Declaration of competing interest

The authors declare that they have no known competing financial interests or personal relationships that could have appeared to influence the work reported in this paper.

Data availability

The raw mass spectrometry data is available under: https://doi.org/10.5281/zenodo.7852039.

Acknowledgment

C.B., C.G., and E.D.V. acknowledge the LUMC fellowship 2020. Figures were partially created in BioRender.com.

Appendix A. Supplementary data

Supplementary data to this article can be found online at https://doi.org/10.1016/j.aca.2023.341795.

References

[1] S.W. de Taeye, T. Rispens, G. Vidarsson, The ligands for human IgG and their effector functions, Antibodies 8 (2) (2019).
[2] G. Vidarsson, G. Dekkers, T. Rispens, IgG subclasses and allotypes: from structure to effector functions, Front. Immunol. 5 (2014) 520.
[3] S.W. de Taeye, A.E.H. Bentlage, M.M. Mebius, J.I. Meesters, S. Lissenberg-Thunnissen, D. Falck, T. Senard, N. Salehi, M. Wuhrer, J. Schuurman, A.F. Labrijn, T. Rispens, G. Vidarsson, FcgammaR binding and ADCC activity of human IgG allotypes, Front. Immunol. 11 (2020) 740.
[4] C. Gstottner, M. Hook, T. Christopeit, A. Knaupp, T. Schlothauer, D. Reusch, M. Haberger, M. Wuhrer, E. Dominguez-Vega, Affinity capillary electrophoresis-mass spectrometry as a tool to unravel proteoform-specific antibody-receptor interactions, Anal. Chem. 93 (45) (2021) 15133–15141.
[5] T.Z. Li, D.J. DiLillo, S. Bournazos, J.P. Giddens, J.V. Ravetch, L.X. Wang, Modulating IgG effector function by Fc glycan engineering, P Natl Acad Sci USA 114 (13) (2017) 3485–3490.
[6] G. Dekkers, L. Treffers, R. Plomp, A.E.H. Bentlage, M. de Boer, C.A.M. Koeleman, S. N. Lissenberg-Thunnissen, R. Visser, M. Brouwer, J.Y. Mok, H. Matlung, T.K. van den Berg, W.J.E. van Esch, T.W. Kuijpers, D. Wouters, T. Rispens, M. Wuhrer, G. Vidarsson, Decoding the human immunoglobulin G-glycan repertoire reveals a spectrum of fc-receptor- and complement-mediated-effector activities, Front. Immunol. 8 (2017).
[7] M. Seeling, C. Bruckner, F. Nimmerjahn, Differential antibody glycosylation in autoimmunity: sweet biomarker or modulator of disease activity? Nat. Rev. Rheumatol. 13 (10) (2017) 621–630.
[8] I. Gudelj, G. Lauc, M. Pezer, Immunoglobulin G glycosylation in aging and diseases, Cell. Immunol. 333 (2018) 65–79.
[9] C. Huhn, M.H. Selman, L.R. Ruhaak, A.M. Deelder, M. Wuhrer, IgG glycosylation analysis, Proteomics 9 (4) (2009) 882–913.
[10] M. Wuhrer, J.C. Stam, F.E. van de Geijn, C.A.M. Koeleman, C.T. Verrips, R.J.E. M. Dolhain, C.H. Hokke, A.M. Deelder, Glycosylation profiling of immunoglobulin G (IgG) subclasses from human serum, Proteomics 7 (22) (2007) 4070–4081.
[11] G. Zauner, M.H. Selman, A. Bondt, Y. Rombouts, D. Blank, A.M. Deelder, M. Wuhrer, Glycoproteomic analysis of antibodies, Mol. Cell. Proteomics 12 (4) (2013) 856–865.
[12] R. Plomp, L.R. Ruhaak, H.W. Uh, K.R. Reiding, M. Selman, J.J. Houwing-Duistermaat, P.E. Slagboom, M. Beekman, M. Wuhrer, Subclass-specific IgG glycosylation is associated with markers of inflammation and metabolic health, Sci Rep-Uk 7 (2017).
[13] M. Haberger, A.K. Heidenreich, M. Hook, J. Fichtl, R. Lang, F. Cymer, M. Adibzadeh, F. Kuhne, H. Wegele, D. Reusch, L. Bonnington, P. Bulau, Multiattribute monitoring of antibody charge variants by cation-exchange chromatography coupled to native mass spectrometry, J. Am. Soc. Mass Spectrom. 32 (8) (2021) 2062–2071.
[14] T. Botzanowski, S. Erb, O. Hernandez-Alba, A. Ehkirch, O. Colas, E. Wagner-Rousset, D. Rabuka, A. Beck, P.M. Drake, S. Cianferani, Insights from native mass spectrometry approaches for top- and middle- level characterization of site-specific antibody-drug conjugates, mAbs 9 (5) (2017) 801–811.
[15] K. Srzentic, L. Fornelli, Y.O. Tsybin, J.A. Loo, H. Seckler, J.N. Agar, L.C. Anderson, D.L. Bai, A. Beck, J.S. Brodbelt, Y.E.M. van der Burgt, J. Chamot-Rooke, S. Chatterjee, Y. Chen, D.J. Clarke, P.O. Danis, J.K. Diedrich, R.A. D'Ippolito, M. Dupre, N. Gasilova, Y. Ge, Y.A. Goo, D.R. Goodlett, S. Greer, K.F. Haselmann, L. He, C.L. Hendrickson, J.D. Hinkle, M.V. Holt, S. Hughes, D.F. Hunt, N. L. Kelleher, A.N. Kozhinov, Z. Lin, C. Malosse, A.G. Marshall, L. Menin, R. J. Millikin, K.O. Nagornov, S. Nicolardi, L. Pasa-Tolic, S. Pengelley, N. R. Quebbemann, A. Resemann, W. Sandoval, R. Sarin, N.D. Schmitt, J. Shabanowitz, J.B. Shaw, M.R. Shortreed, L.M. Smith, F. Sobott, D. Suckau, T. Toby, C.R. Weisbrod, N.C. Wildburger, J.R. Yates 3rd, S.H. Yoon, N.L. Young, M. Zhou, Interlaboratory study for characterizing monoclonal antibodies by top-down and middle-down mass spectrometry, J. Am. Soc. Mass Spectrom. 31 (9) (2020) 1783–1802.
[16] B.L. Duivelshof, A. Beck, D. Guillarme, V. D'Atri, Bispecific antibody characterization by a combination of intact and site-specific/chain-specific LC/MS techniques, Talanta 236 (2022).
[17] J. Kim, L. Jones, L. Taylor, G. Kannan, F. Jackson, H. Lau, R.F. Latypov, B. Bailey, Characterization of a unique IgG1 mAb CEX profile by limited Lys-C proteolysis/CEX separation coupled with mass spectrometry and structural analysis, J. Chromatogr., B: Anal. Technol. Biomed. Life Sci. 878 (22) (2010) 1973–1981.
[18] J. Sjogren, F. Olsson, A. Beck, Rapid and improved characterization of therapeutic antibodies and antibody related products using IdeS digestion and subunit analysis, Analyst 141 (11) (2016) 3114–3125.
[19] C. Blochl, C. Regl, C.G. Huber, P. Winter, R. Weiss, T. Wohlschlager, Towards middle-up analysis of polyclonal antibodies: subclass-specific N-glycosylation profiling of murine immunoglobulin G (IgG) by means of HPLC-MS, Sci. Rep. 10 (1) (2020), 18080.
[20] B.L. Duivelshof, S. Denorme, K. Sandra, X. Liu, A. Beck, M.A. Lauber, D. Guillarme, V. D'Atri, Quantitative N-glycan profiling of therapeutic monoclonal antibodies performed by middle-up level HILIC-HRMS analysis, Pharmaceutics 13 (11) (2021).
[21] A.M. Goetze, Z.Q. Zhang, L. Liu, F.W. Jacobsen, G.C. Flynn, Rapid LC-MS screening for IgG Fc modifications and allelic variants in blood, Mol. Immunol. 49 (1–2) (2011) 338–352.
[22] T. Senard, A.F.G. Gargano, D. Falck, S.W. de Taeye, T. Rispens, G. Vidarsson, M. Wuhrer, G.W. Somsen, E. Dominguez-Vega, MS-based allotype-specific analysis of polyclonal IgG-Fc N-glycosylation, Front. Immunol. 11 (2020) 2049.
[23] U. Schauer, F. Stemberg, C.H.L. Rieger, M. Borte, S. Schubert, F. Riedel, U. Herz, H. Renz, M. Wick, H.D. Carr-Smith, A.R. Bradwell, W. Herzog, IgG subclass concentrations in certified reference material 470 and reference values for children and adults determined with the binding site reagents, Clin. Chem. 49 (11) (2003) 1924–1929.
[24] B. MacLean, D.M. Tomazela, N. Shulman, M. Chambers, G.L. Finney, B. Frewen, R. Kern, D.L. Tabb, D.C. Liebler, M.J. MacCoss, Skyline: an open source document editor for creating and analyzing targeted proteomics experiments, Bioinformatics 26 (7) (2010) 966–968.
[25] R. Adusumilli, P. Mallick, Data conversion with ProteoWizard msConvert, Methods Mol. Biol. 1550 (2017) 339–368.
[26] H.L. Rost, T. Sachsenberg, S. Aiche, C. Bielow, H. Weisser, F. Aicheler, S. Andreotti, H.C. Ehrlich, P. Gutenbrunner, E. Kenar, X. Liang, S. Nahnsen, L. Nilse, J. Pfeuffer, G. Rosenberger, M. Rurik, U. Schmitt, J. Veit, M. Walzer, D. Wojnar, W.E. Wolski, O. Schilling, J.S. Choudhary, L. Malmstrom, R. Aebersold, K. Reinert, O. Kohlbacher, OpenMS: a flexible open-source software platform for mass spectrometry data analysis, Nat. Methods 13 (9) (2016) 741–748.
[27] R Core Team, R: A Language and Environment for Statistical Computing, R Foundation for Statistical Computing, Vienna, Austria, 2013. http://www.R-project.org/.
[28] M.-P. Lefranc, G. Lefranc, Human Gm, Km, and Am Allotypes and Their Molecular Characterization: a Remarkable Demonstration of Polymorphism, Immunogenetics, Springer, 2012, pp. 635–680.
[29] E. Ossipova, C.F. Cerqueira, E. Reed, N. Kharlamova, L. Israelsson, R. Holmdahl, K. S. Nandakumar, M. Engstrom, U. Harre, G. Schett, A.I. Catrina, V. Malmstrom, Y. Sommarin, L. Klareskog, P.J. Jakobsson, K. Lundberg, Affinity purified anti-citrullinated protein/peptide antibodies target antigens expressed in the rheumatoid joint, Arthritis Res. Ther. 16 (4) (2014).
[30] D. Falck, M. Thomann, M. Lechmann, C.A.M. Koeleman, S. Malik, C. Jany, M. Wuhrer, D. Reusch, Glycoform-resolved pharmacokinetic studies in a rat model employing glycoengineered variants of a therapeutic monoclonal antibody, mAbs 13 (1) (2021).

[31] R. Jefferis, M.P. Lefranc, Human immunoglobulin allotypes: possible implications for immunogenicity, mAbs 1 (4) (2009) 332–338.
[32] H. Liu, G. Ponniah, H.M. Zhang, C. Nowak, A. Neill, N. Gonzalez-Lopez, R. Patel, G. Cheng, A.Z. Kita, B. Andrien, In vitro and in vivo modifications of recombinant and human IgG antibodies, mAbs 6 (5) (2014) 1145–1154.
[33] C. Regl, T. Wohlschlager, J. Holzmann, C.G. Huber, A generic HPLC method for absolute quantification of oxidation in monoclonal antibodies and Fc-fusion proteins using UV and MS detection, Anal. Chem. 89 (16) (2017) 8391–8398.
[34] M. Landon, Cleavage at aspartyl-prolyl bonds, in: Methods in Enzymology, Elsevier, 1977, pp. 145–149.
[35] K. Stavenhagen, R. Plomp, M. Wuhrer, Site-specific protein N- and O-glycosylation analysis by a C18-porous graphitized carbon-liquid chromatography-electrospray ionization mass spectrometry approach using pronase treated glycopeptides, Anal. Chem. 87 (23) (2015) 11691–11699.
[36] C. Gstottner, T. Zhang, A. Resemann, S. Ruben, S. Pengelley, D. Suckau, T. Welsink, M. Wuhrer, E. Dominguez-Vega, Structural and functional characterization of SARS-CoV-2 RBD domains produced in mammalian cells, Anal. Chem. 93 (17) (2021) 6839–6847.
[37] Y. Yang, F. Liu, V. Franc, L.A. Halim, H. Schellekens, A.J.R. Heck, Hybrid mass spectrometry approaches in glycoprotein analysis and their usage in scoring biosimilarity, Nat. Commun. 7 (2016).
[38] A. Lapolla, D. Fedele, M. Garbeglio, L. Martano, R. Tonani, R. Seraglia, D. Favretto, M.A. Fedrigo, P. Traldi, Matrix-assisted laser desorption/ionization mass spectrometry, enzymatic digestion, and molecular modeling in the study of nonenzymatic glycation of IgG, J. Am. Soc. Mass Spectrom. 11 (2) (2000) 153–159.
[39] P.M. Danze, A. Tarjoman, J. Rousseaux, P. Fossati, M. Dautrevaux, Evidence for an increased glycation of IgG in diabetic patients, Clin. Chim. Acta 166 (2–3) (1987) 143–153.
[40] H. Sarvas, N. Rautonen, H. Kayhty, M. Kallio, O. Makela, Effect of gm allotypes on Igg2 antibody-responses and Igg2 concentrations in children and adults, Int. Immunol. 2 (4) (1990) 317–322.